Antenna Measurement Implementations and Dynamic Positional Validation Using a Six Axis Robot[1]

David R. Novotny†, Joshua A. Gordon, Michael Francis, Ronald Wittmann, Alexandra Curtin, Jeffrey Guerrieri
Communications Technology Laboratory
National Institute of Standards and Technology
Boulder, CO, United States of America
†david.novotny@nist.gov

***Abstract*—We have performed spherical and extrapolation scans of two antennas at 118 GHz using a commercial 6-axis robot. Unlike spherical scanning, linear extrapolations do not precisely conform to the natural circular movement about individual robot axes. To characterize the quality of the data, we performed dynamic position and orientation characterization of the robotic systems. A laser tracker is used to measure the probe antenna movement relative to the antenna under test, this information is used to continually update the position and posture of the probe during scanning. We correlated the laser tracker data with the mmWave insertion phase to validate dynamic measurement position results at speeds up to 11 mm/s. We previously demonstrated spherical measurements with this system. The extrapolation measurements presented here require more stringent accuracies for pointing that general pattern analysis.**

I. INTRODUCTION

Higher frequencies, multiple geometries, many antennas, multiple frequencies, rapid beam state changes, shorter testing requirements…. We are attempting to address many of these antenna testing issues simultaneously.

There are requirements to test at higher frequencies for climate, security, and communications applications that need tighter tolerances on positioning, orientation and timing between system components than at lower frequencies. The ability to test multiple geometries such as planar scans at various orientations, or a spherical and extrapolation measurement with one setup, may allow for more rigorous testing with minimal increases in test time. We now see cell phones and spacecraft with many operational antennas that may need to be tested independently and having a test facility that can accommodate multiple testing requirements (NFC, Bluetooth, GPS, Cellular & Wi-Fi), might prove valuable. Finally, the ability to rapidly move probe antennas around test objects while maintaining orientation relative to the object under test may have applications in dynamic antenna testing and conformal testing such as medical and shielding applications.

The use of coordinated robotics with multiple degrees of freedom and using laser-based positioning metrology equipment to guide and correct the scan geometries may offer solutions to these antenna testing issues.

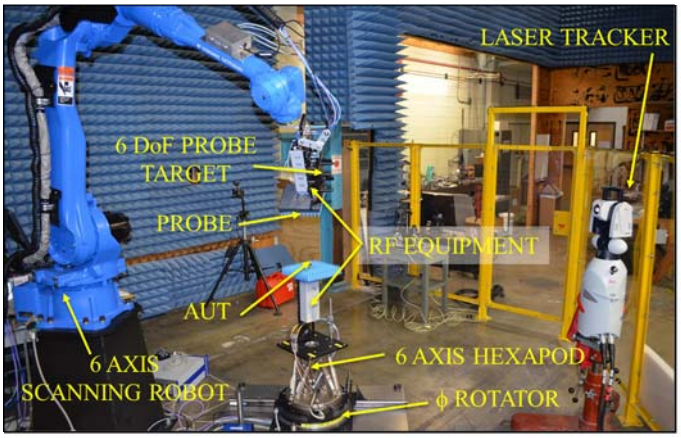

Figure 1. Major components of the Configurable MilliMeter Robotic Antenna Facility (CROMMA).

II. OVERVIEW

Previously, the Antenna Metrology project at NIST and others have presented results of mmWave spherical scanning using a six Degree-or Freedom (6DoF) robotic system [1,2]. The Configurable Robotic MilliMeter Antenna facility (CROMMA), fig. 1, has produced pattern and imaging measurement results from 60 to 225 GHz [1,3].

The major goal of this endeavor is to develop a configurable platform that can use different measurement geometries with minimal setup and alignment. The 6DoF positioning capabilities of the antenna under test (AUT) and probe stages, guided by the laser tracker, allow for correcting both pointing and positioning throughout the scan geometry with minimal alignment effort between the antenna and positioner.

We continue to explore the ability of commercial-off-the-shelf (COTS) hardware to perform high accuracy testing. There is a lively debate on the practical ability to perform large volumetric scans using conventional mmWave measurement equipment [4,5]. Both positioning of the antennae and mmWave stability need to be determined to assess the quality of the entire measurement. If there is a considerable amount of variation in mmWave phase or amplitude (e.g. due to cable flexing or temperature shifts) then significant errors may be seen in the calculated antenna parameters. Similarly, if the quality of

position data from the laser tracker degrades when the target changes speed, resulting position errors translate directly into pattern and gain errors.

We are currently focusing on the quantification of errors in the CROMMA facility for multiple measurements types. In this paper, we concentrate on how one setup, which involves locating the probe and AUT relative to their robotic stages and laser tracker targets, can be used for multiple geometry testing. High frequency testing requires positioning accuracies on the order of λ/25 to λ/50. So at 118 GHz, with a wavelength, λ, of approximately 2.5 mm, we may desire positional accuracies on the order of 50 to 100 µm. Pointing accuracies are generally more antenna than frequency dependent: knowledge of the pointing angle to 1/50th of the expected beam-width is a starting point. With such tight mechanical tolerances, coordinating the mmWave measurement, the robotic path, and measurement of the antenna position is critical. Finally, many laser trackers are not quantified for measurements while the target is moving, so the dynamic accuracy of the laser tracker itself needs to be determined.

To support an upcoming test for a climate radiometer, we performed antenna tests at approximately 118 GHz, using a 15 dBi standard gain horn as the probe antenna and a 9 dBi, µ=±1 antenna as the AUT. We performed a spherical scan followed by an extrapolation measurement using only one antenna alignment. We calibrated the robotic path for each geometry and updated the path during the measurement to account for robot warmup and mechanical drift. During the extrapolation measurement, we compared the mmWave phase measurement, translated to distance, to the laser tracker measured distance.

III. CROMMA

The use of coordinated-motion robotics for antenna and imaging techniques is being explored by several groups and manufacturers. Full 6DoF positioning has great possibilities for reducing errors that independent stacked stages of earlier generations of antenna positioning systems employ. However, while many of the modern day 6- and 7-axis robots are very repeatable, they are not always very accurate. CROMMA, fig. 1, uses laser trackers to locate the antennas relative to the robotic stages, relative to other antenna locations and most importantly, relative to the positional measurement targets used to infer antenna position[6].

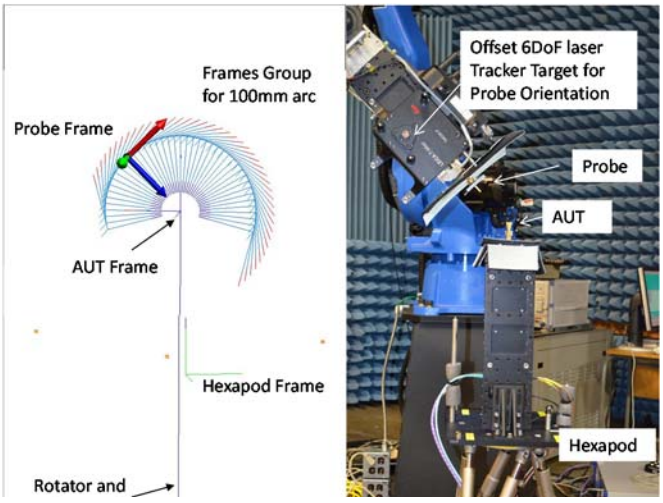

Figure 2. The modeled (left) and actual (right) layout of the CROMMA. The actual locations of each part of the system have been measured by the laser tracker to facilitate alignment and measurements.

We locate all the components within CROMMA using the laser tracker: the base φ rotator axis, the hexapod's coordinate frame and the robot's base movement frame, fig. 2. We measured the location of the antennas with an absolute-position, single-pixel camera target [6] and simultaneously aligned the antennas to the robot and rotator using the robot's tool tip calibration procedure and direct hexapod movement.

We start with an ideal scan geometry using the native robotic coordinate system. The laser tracker sends position and pointing error data back to the coordinate metrology software and it is used to continuously improve robotic positioning performance throughout the measurement, fig. 2.

Continuous correction is needed to achieve the best possible positioning accuracies of the system. If accuracies on the order of base robot repeatability are acceptable, in our case, approximately 70 µm [7], then continuous laser-tracker feedback is not required. Large volume, periodic, 6DoF robotic calibration that can maintain validity for many months has been used to correct robot accuracy to approximately the robotic repeatability specification [8]. For lower frequency applications or those not requiring such stringent positioning specifications, laser tracker data throughout the measurements may not be needed. Though, it can be shown that position data from an imperfect scan can be used to improve the final pattern data [9].

IV. THE DYNAMIC PROBLEM

Most antenna measurements are taken "on-the-fly", or while either the probe or AUT are moving. This is done to reduce measurement time. However we are trying to accurately locate

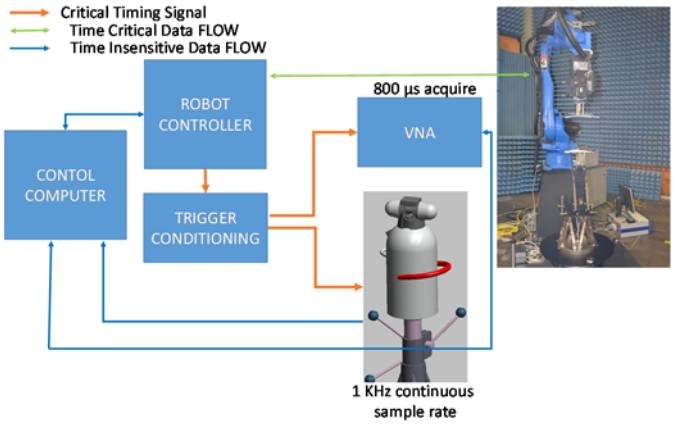

Figure 3. System timing diagram for the CROMMA. The robot controller generates the timing pulse prior to reaching a programmed position. The pusle is delayed and amplitude adjusted for the VNA and the laser tracker. Position and mmWave data is queued and retrived by the computer in a non-time critical serivce loop.

the antennas to roughly the accuracy of the laser tracker, ~±20 µm, while the antenna is moving and coordinate it with the mmWave transmission measurement. Compounding the problem: the instrument we rely on for scan correction, the laser tracker, does not have a test for or specifications on dynamic accuracy. So we will attempt to break the problem into two sections: the mmWave measurement errors and then the comparison between the mmWave and optical measurement of position.

A. Sysetem Timing Setup.

Timing between robot positioner, the laser tracker and the Vector Network Analyzer (VNA) is critical to maintaining the desired accuracy. To maintain minimal operating system delays, the robot is used to generate the main timing signal, fig 3. It generates a pulse prior to arriving at a programmed point and that signal is delayed and distributed to the laser tracker and VNA so the position data is taken at the midpoint of the mmWave measurement. Data is transferred to the robot and from the laser tracker and VNA via non-time-critical queues.

Characterization of the laser tracker timing is critical. The VNA timing is well characterized, timing uncertainties are specified as less than 12.5 ns [10]. Trigger conditioning adds less than 3 ns jitter. So the measurement of the mmWave data is well coordinated in time. The laser tracker polls the elevation and azimuth encoders (1 KHz), distance interferometer (1 KHz), and orientation sensors (250 Hz) continuously at different rates and interpolating between samples depending on the trigger arrival.

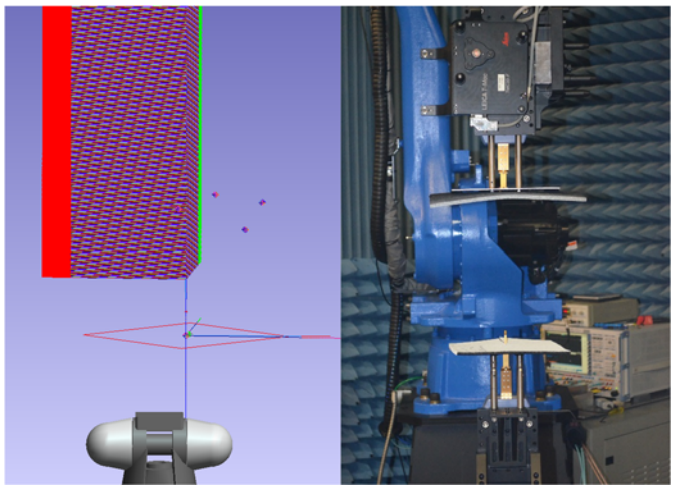

Figure 4. Extrapolation path used in this measurement. The robot taking data in 0.84 mm (λ/3) steps. The path is corrected to maintain proper pointing throughout the measurement.

B. mmWave tracking errors.

We performed an extrapolation measurement to compare the timing and dynamic position accuracy of the laser tracker versus the VNA, fig. 4. We performed a linear scan from 50 mm ($\sim 2D^2/\lambda$) to 600 mm ($\sim 24D^2/\lambda$). We corrected the path until we attained optimal pointing and positioning errors, fig. 5.

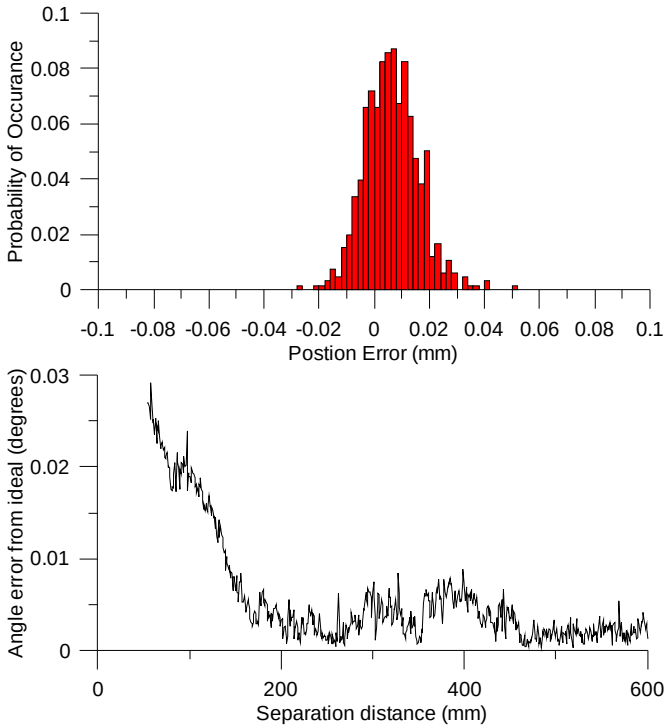

Figure 5. Histogram of position errors (upper) and angular errors along the path (lower) for the extrapolation measurement after path correction. The rise at small distances is due to polarization rotation because of the angle to the 6DoF sensor.

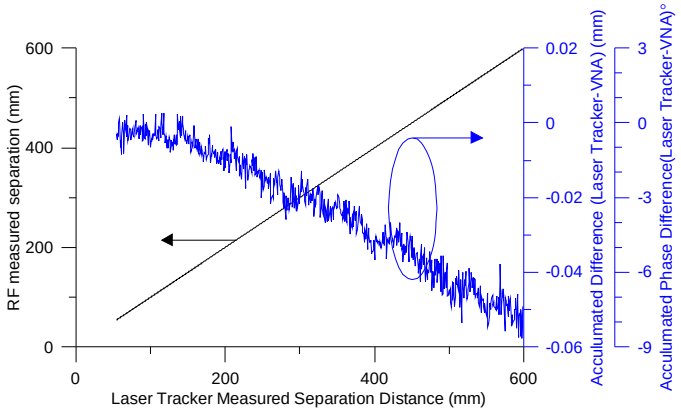

Figure 6. Distance between antennas as measured by the laser tracker and the VNA at a robot speed of 1 mm/s. A difference of ~8° over a 600mm linear separation is mainly attributed to cable flexure. The inherent positional noise is approximately 10 µm which is a combination of the VNA and laser tracker.

In order to use the mmWave analyzer as a basis for comparing with the laser tracker, we need to perform a basic assessment on the stability of the mmWave system. The two most prominent sources of mmWave stability errors are cable movement and temperature. The temperature in the laboratory is regulated to ±2 C, so we expect minimal thermal drift in the VNA. By running the cables along the robot's control cable path, we previously showed single point position repeatability of 25 µm, with mmWave repeatability of 7° and 0.02 dB [4]. For this measurement we looked at unwrapped phase and used it to

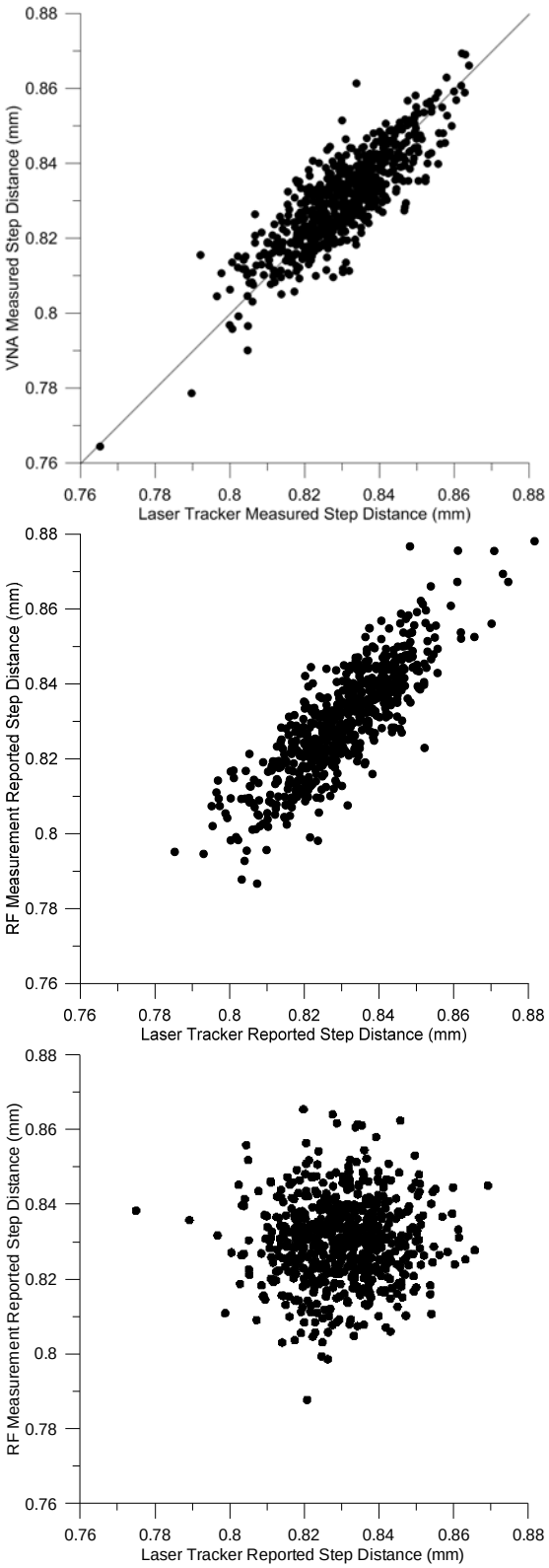

Figure 7. Measurements of VNA reported step size vs the laser tracker reported step at three speeds (ideal step 0.842 mm). At 1.1 mm/s (top) we see very good correlation. At 3.5 mm/s (middle) correlation is reduced. At 11.0 mm/s (bottom) we lose 1-1 correlation but we have tighter control over position variation.

infer distance. We compared the results with the reported laser tracker position and compared the differences, fig. 6. We see a systematic phase progression as the cable moves which imparts an offset, linear with distance, of about 8° or 50 µm over the 550 mm scan. This error level of 10^{-4} or -40 dB and the phase correlation between the tracker and the VNA show that the system is nominally stable enough with movement to perform varying velocity scans.

C. *Dymanic Accuracy at varying veloicities.*

Since the slow movement showed high correlation between mmWave and tracker measurements, we increased speed of separation between the probe and the AUT. Fig. 7 shows the reported step size by the VNA compared to the laser tracker at speeds of 1.1, 3.5 and 11 mm/s. The laser tracker is sampling data constantly and outputs an interpolated position between samples based on the arrival of the trigger [11]. The VNA was setup with a 1 KHz IFBW, which averages mmWave data for approximately 800 µs. We see very good distance correlation between the VNA and Laser Tracker when not moving or at slow speeds (1.1 mm/s). The correlation in positon gets slightly worse at 3.5 mm/s but agreement is generally still within ±10 µm RMS. At 11 mm/s the fine correlation in position is lost but the tracker and VNA are still reading within ±20 µm. at 11 mm/s The antennas move approximately 9.9 µm during the course of the VNA measurement, Table 1. The averaging of phase over this travel could cause a large portion of the loss in correlation. The speeds examined here are relatively slow for production line measurements, however, they do show that at these speeds, the laser tracker is producing results consistent with an independent instrument. Further work will decrease the VNA averaging time and increase the speed of the scan.

V. MMWAVE ANTENNA RESULTS

The overarching goal for CROMMA is to measure antenna parameters such as gain and pattern. We performed an

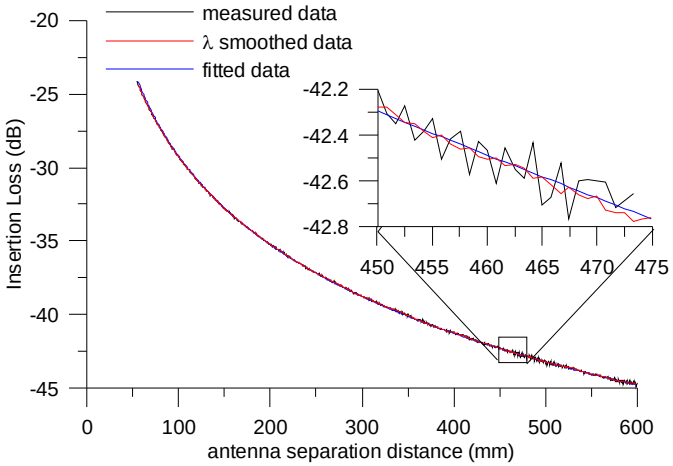

Figure 8. Plot of extrapolation data at 118 GHz for the µ±1 probe vs a 15 dBi standard gain horn. The data spans a $2D^2/\lambda$ to $24D^2/\lambda$ range, there is little evidence of exterior reflections until a spacing of 450 mm which is removed by the wavelength level smoothing.

extrapolation scan at approximately 118 GHz, followed by three far-field spherical scans at approximately 112, 118 and 125 GHz, all using the same antenna alignment. The patterns were measured at a radius of 100 mm, or at approximately twice the nominal far-field criterion of $2D^2/\lambda$.

The extrapolation was performed for only one pair of antennas, fig. 8, so we can only calculate combined pair gain, $G_P G_{AUT}$, for the Probe, G_P, and AUT, G_{AUT}. A simple fit with distance, R, to the far-field Friis transmission formula:

$$\frac{P_r}{P_t} = S_{21} = G_P G_{AUT} \left(\frac{\lambda}{4\pi R}\right)^2 |\alpha_P \cdot \alpha_{AUT}{}^*|^2 [M]$$

where $\alpha_P \cdot \alpha_{AUT}$ is the polarization mismatch and, $[M]$, is generated from the mismatch the antenna ports, yields the pair gain, fig. 8. The reflection mismatch is accounted for by the full two port-calibration, and the polarization mismatch is minimal with the small angular errors. The confiniment of phase also shows that we are in a valid range of fitting to far-field paramenters [12]. Table 1, summarizes the gain caclualted for each velocity sweep.

TABLE I. EXTRAPOLATION RESULTS.

Probe Speed	**1.1 mm/s**	**3.5 mm/s**	**11.0 mm/s**
Movement during VNA measurement	1 µm	3.1 µm	9.9 µm
Movement during LT measurement	.4 µm	1.2 µm	3.6 µm
$G_P G_{AUT}$ Pair Gain (dB)	24.69	24.70	24.62
uncertianity	±0.1 dB	±0.1 dB	±0.1 dB

The far-field pattern measurements of the µ=±1 antenna, fig. 9, show minimal change across the frequency band of interest (<0.4 dB change in relative peak level). And less than 1° change in the -6 dB beam width.

The cross polarization pattern measurements show that cross polarization can't be accurately determined in the far-field. We only have approximately 80 dB of dynamic range at 118 GHz. The nominal insertion loss on boresight from the extrapolation measurements, fig. 8, is approximately -39.4 dB at 100 mm. This leaves only 40 dB of measurement sensitivity. Decreasing the measurement radius and performing a full spherical near-field analysis is needed to fully determine the antenna pattern.

VI. CONCLUSIONS

We have demonstrated that the CROMMA is capable of accuratly scanning multiple geometries. The 6DoF robotic arm naturally operates in circular motion which is optimal for spherical and cylindrical scanning. However, we have shown that fine control allows for effective linear motion on the order of at least 20 µm accuracy. Using the λ/50 rule, this allows for linear motion needed for planar and extrapolation scanning to at least 300 GHz.

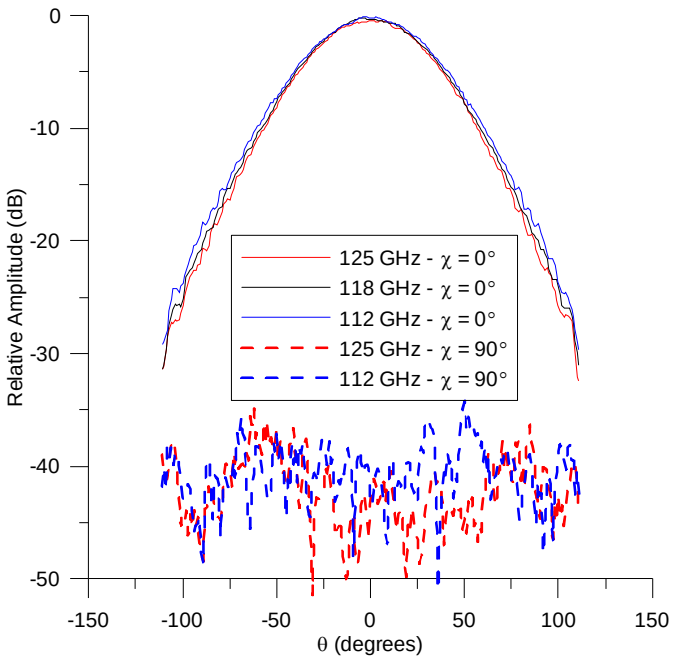

Figure 9. Far-field spherical data at three frequencies. At 100 mm, ~ $4D^2/\lambda$, the χ = 0° peaks are within 0.5 dB. The cross-polarized data for the probe is below the -40 dB limit of the measurement system to detect.

Additionally, we have demonstrated the dynamic accuracy of the laser tracker used to guide the robot during the scan. Previously, the accuracy of the tracker was only specified for static measurements. These three pieces, the demonstrated 6DoF scan capability, the mmWave stability and the validated, dynamic tracking "close the loop" and allow the confident use of these 6DoF systems for arbitrary antenna scan geometers at high frequencies. Use of these systems, once characterized [8], at lower frequencies, without the use of a laser tracker, can generate precise patterns with λ/50 accuracy.

Future work will concentrate on increasing the scanning speed of the system and testing high performance antennas. We would like to extend the capabilities to the *dynamic* testing of beamforming antennas. Tests such as measurement of side lobes and spurious emissions as main beams scan or track targets, or *in-situ* testing of multi-beam systems using user-equipment emulation systems as probes.

REFERENCES

[1] J. A. Gordon, D. R. Novotny, J. B. Coder, J. R. Guerrieri, B. Stillwell, "Robotically controlled mm-wave near-field pattern range," Proceedings of the 2012 Antenna Measurement Techniques Association., Nov 2012.

[2] L. Boehm, F. Boegelsack, M. Hitzler, C. Waldschmidt, "An automated millimeter-wave antenna measurement setup using a robotic arm," 2015 IEEE International Symposium on Antennas and Propagation and North American Radio Science Meeting, TUP-A1.5A.7, 19-24 July 2015.

[3] M. H. Francis, R. C. Wittmann, D. R. Novotny, J. A. Gordon, ”Spherical near-field measurement results at millimeter-wave frequencies using robotic positioning,” Proceedings of the 2014 Antenna Measurement Techniques Association, Oct 2014.

[4] D. R. Novotny, J. A. Gordon, J. R. Guerrieri, “Antenna alignment and positional validation of a mmWave antenna system using 6D coordinate metrology,” Proceedings of the 2014 Antenna Measurement Techniques Association, Oct 2014.

[5] M. Hitzler, S. Bader, C. Waldschmidt, "Key aspects of robot based antenna measurements at millimeter wave frequencies," Antennas and Propagation (EuCAP), 2014 8th European Conference on , vol., no., pp.392,396, 6-11 April 2014.

[6] J.A. Gordon, D.R. Novotny, “A Non-Contact Machine Vision System for the Precision Alignment of mm-Wave Antennas in all Six Degrees of Freedom,” Proceedings of the 2014 Antenna Measurement Techniques Association, Oct 2014.

[7] Motoman/Yaskawa MH50 / MH50-35 Datasheet, avialble at http://www.motoman.com.

[8] T. Nielsen, S. Sandwidth,”Production line robot calibration verification test results,” Proceedings of the Coordinate Metrology Society Conference, July 2015.

[9] R. C. Wittmann, M. H. Francis, J. A. Gordon, D. Novotny, “Generalized probe-position compensation methods for near-field antenna measurements,” Proceedings of the 2015 Antenna Measurement Techniques Association, Oct 2015, unpublished.

[10] “R&S® ZVA Vector Network Analyzer: Specifications”. Version 13.02 May 2015. Avialabe at http://www.rohde-schwarz.us.

[11] “Leica Tracker Programming Interface: Programmers Manual: Tracker Trigger Interface,” Version 3.6, August 21,2009.

[12] J. B. Coder, D. R. Novotny, M. H. Francis, J. R. Guerrieri, “On the use of phase data when conducting an extrapolation measurement,” Proceedings of the 2013 Antenna Measurement Techniques Association, Nov 2013.